




Heat capacity, thermal expansion and barocaloric effect in fluoride K_2TaF_7

I. N. Flerov^{1,2,*} , M. V. Gorev^{1,2}, A. V. Kartashev^{1,3}, E. I. Pogorel'tsev^{1,2}, and N. M. Laptash⁴

¹Kirensky Institute of Physics, Federal Research Center KSC Siberian Branch, Russian Academy of Sciences, Krasnoyarsk, Russia 660036

²Institute of Engineering Physics and Radioelectronics, Siberian Federal University, Krasnoyarsk, Russia 660074

³Astafijev Krasnoyarsk State Pedagogical University, Krasnoyarsk, Russia 660049

⁴Institute of Chemistry, Far East Branch, Russian Academy of Sciences, Vladivostok, Russia 690022

Received: 4 July 2019

Accepted: 10 August 2019

Published online:
22 August 2019

© Springer Science+Business Media, LLC, part of Springer Nature 2019

ABSTRACT

The heat capacity and thermal expansion of potassium heptafluorotantalate were studied. The room temperature phase $P2_1/c$ is stable at least to 4 K. The strong first-order phase transition $P2_1/c - Pnma$ at $T_0 = 486.2$ K is accompanied by giant changes in the entropy, $\Delta S_0 = 22.3$ J (mol K)⁻¹, and volume strain, $\delta V_0/V = -3.6\%$. A rather high sensitivity of K_2TaF_7 to pressure was found, $dT_0/dp = -220$ K G Pa⁻¹. Significant extensive and intensive barocaloric effects are found at low pressure. The possibility of improving the barocaloric properties is discussed.

Introduction

The shape of the anionic polyhedron in complex inorganic fluorides can be rather different depending on the valency and size of the central atom and plays an important role in the formation of a crystal lattice and the physical properties of its compounds [1]. Octahedral anions MF_6^{m-} are the most frequent structural building units. However, there are also many compounds with other forms of fluorine polyhedron. For example, the structure of fluorides with the general chemical formula A_2MeF_7 consists of the seven-coordinated MeF_7^{2-} anionic complex in the form of a monocapped trigonal prism with C_{2v} symmetry [2].

Heptafluorides A_2TaF_7 (A: K, NH_4 , Rb) belonging to this series of crystals are characterized by different room temperature symmetries of the crystal lattice, depending on the size of the monovalent cation A. While compounds with A = Rb, NH_4 have tetragonal symmetry ($P4/nmm$, $Z = 2$) [3], potassium heptafluorotantalate is monoclinic ($P2_1/c$, $Z = 4$) [2, 4]. The crystal lattice stabilities of heptafluorides with respect to temperature change also differ. The tetragonal phase of the first two crystals is stable when heated to the decomposition temperature. Upon cooling, both compounds undergo unique and successive phase transitions: $Rb_2TaF_7 - P4/nmm$ ($T_0 = 145$ K) – $Cmma$ [5]; $(NH_4)_2TaF_7 - P4/nmm$ ($T_1 = 174$ K) – $Pmmm$ ($T_2 = 156$ K) – tetragonal [6]. In accordance

Address correspondence to E-mail: flerov@iph.krasn.ru

with the small values of the corresponding entropy change ($\Delta S \leq 0.5R$), all of these transformations have been considered as belonging to the displacive type [5, 6].

The monoclinic phase in K_2TaF_7 remains stable when cooled to at least 100 K [7], and, upon heating, potassium heptafluorotantalate undergoes two structural phase transitions [8]. One of them takes place at 998 K, which is very close to the point of the incongruent melting at 1022 K and is accompanied by mass loss. This is the reason why the main attention of investigators is usually paid to the reverse structural transformation $P2_1/c$ ($T_0 = 475$ K) – $Pnma$ ($Z = 4$) [4], which is rather unusual due to the following intriguing points. (1) The space groups $P2_1/c$ and $Pnma$ are connected by the group–subgroup relation. However, the large structural distortions in the monoclinic phase and huge thermal hysteresis found [8] are typical of a reconstructive phase transition. (2) Despite the absence of structural disorder in the phase $Pnma$ [9], a large entropy change, $\Delta S = R \ln 6$, obtained using a differential scanning calorimeter (DSC), is characteristic of order–disorder transformations [8]. This contradiction can be explained by taking into account a giant change in the volume of the anionic polyhedron as well as the coordination number of the central atom Ta. (3) The origin of the structural distortions has been characterized as ‘proper’ ferroelastic, and a significant change in the phase transition parameter η has been found for a wide range of temperatures below T_0 . But, the temperature-dependent part of the corresponding entropy $\Delta S(T) \sim \eta^2(T)$ was detected in DSC measurements only in a rather narrow temperature region [8]. (4) Heat treatment causes changes in the temperature and enthalpy of the phase transition, but does not change the corresponding entropy [7].

Due to the large change in entropy during the phase transition, it is possible to assume that K_2TaF_7 has a very high barocaloric efficiency. However, to analyse the intensive and extensive barocaloric effects (BCEs), detailed information is needed on the temperature dependencies of the entropy and elastic deformation, as well as on the sensitivity of the temperature of the phase transition to external pressure.

In the present paper, we present the results of a thorough study of the heat capacity and thermal expansion over a wide temperature range, which has

allowed determining the main thermodynamic parameters of the phase transition $P2_1/c - Pnma$. We also evaluated the baric coefficient, dT_0/dp , characterizing the stability of the crystal lattice with respect to hydrostatic pressure as well as the intensive ΔT_{AD} and extensive ΔS_{BCE} BCE.

Sample preparation and measurement technique

Sample preparation and characterization

Potassium heptafluorotantalate was prepared by its precipitation from a solution of hydrofluoric acid. A starting material, Ta_2O_5 , of reagent grade, was dissolved in concentrated HF (40% wt) with heating followed by the addition of KCl. A stoichiometric quantity of potassium salt was added to the solution diluted with water in accordance with the reaction $H_2TaF_7 + 2KCl = K_2TaF_7 + 2HCl$. The crystalline precipitate was filtered and washed under vacuum with alcohol. Using EDX and XPS methods, the composition of the crystals was checked. Both indicated the presence of oxygen. The amount of fluorine was determined by a fluoride ion-selective electrode calibrated with variously diluted solutions of standard NaF. The real content of fluorine was $31.5 \pm 0.4\%$ (compared to the calculated 33.92% for K_2TaF_7). Thus, the composition of the crystals grown is $K_2TaO_{0.3}F_{6.4}$.

X-ray studies were performed to make sure that such an amount of oxygen impurity does not affect the type of structure. All peaks on the powder diffraction patterns were indexed by monoclinic cell $P2_1/c$ with parameters close to those previously found for K_2TaF_7 [2, 10]. This crystal structure was taken as the starting model for Rietveld refinement, which was found to be stable, revealing low R -factors ($R_{wp} = 5.81\%$, $R_p = 4.64\%$, $\chi^2 = 1.63$). Thus, we can use the stoichiometric formula K_2TaF_7 .

Dilatometry

Measuring the thermal expansion was accomplished using a push-rod dilatometer (NETZSCH model DIL-402C) with a fused silica sample holder. The experiments were carried out in the temperature range of 100–750 K with a heating rate of 3 K min^{-1} in a dry He flux. The results were calibrated by taking quartz

as the standard reference, in order to eliminate the influence of the thermal expansion of the system. The reproducibility of the data obtained in all successive series of measurements was not less than 5%. Samples for dilatometric measurements were prepared as quasi-ceramic disc-shaped pellets with a diameter of 6 mm and a thickness of 1.3 mm.

Calorimetry

Detailed measurements of the heat capacity, $C_p(T)$, of K_2TaF_7 were performed in a wide temperature range of 4–600 K by means of three calorimetric methods.

Below 90 K, the dependence $C_p(T)$ was studied using a special option of a Physical Property Measurement System (PPMS, Quantum Design, USA). The measurements were performed on a ceramic sample. Apiezon N grease was used to provide reliable thermal contact between the sample and the additives. The relative error of measurements was less than 1%.

A homemade adiabatic calorimeter with three screens, as described in Ref. [11], was used in the experiments between 80 and 320 K. The heat capacity of the ‘sample + heater + contact grease’ system was measured using discrete as well as continuous heating. In the former case, the temperature step was varied from 1.5 to 3.0 K. In the latter case, the system was heated at rates of about 0.15–0.30 K min⁻¹. The heat capacities of the heater and contact grease were determined in individual experiments. The inaccuracy in the heat capacity determination did not exceed 0.5–1.0%.

The high-temperature heat capacity was measured by DSC on a NETZSCH 204 F1 instrument in a dry helium flow (20 ml min⁻¹) in the temperature range 300–600 K at a heating rate of 5 K min⁻¹ with an accuracy of ~2%. Sapphire was used as the standard.

Results and discussion

Thermal expansion

The results of two consecutive dilatometric experiments are presented in Fig. 1. In the first heating mode, the measurements were started from 100 K. The temperature behaviour of the coefficient of volume thermal expansion, β , and volumetric strain, $\Delta V/V = 3(\Delta L/L)$, shows only one anomaly at

$T_0 = 486 \pm 1$ K. According to the very large value of the thermal hysteresis $\delta T_0 \approx 50$ K [8], the phase transition should take place upon cooling at 436 K. Due to the specific features of the dilatometric installation, measurements in the cooling mode can be carried out only down to ~450 K, and as a result, no anomalies were detected upon cooling. During the second heating, started from 300 K, a more pronounced negative anomaly $\Delta\beta$ was observed, which is about two times larger than the anomaly during the first heating. The observed difference may be due to the residual mechanical stresses arising in the quasi-ceramic sample during its preparation and annealing during the first heating to 750 K.

In accordance with the first-order $Pnma - P2_1/c$ transformation, strong anomalous behaviour in the volume strain was observed in the narrow temperature range around T_0 with a negative strain jump of $\delta V_0/V = -(36 \pm 5) \times 10^{-3}$ (Fig. 1b). This value gives the dominant contribution to the total change in the volume strain and clearly indicates that the phase transition is far from the tricritical point where $\delta V_0/V \rightarrow 0$.

Heat capacity

Good agreement was found between the results of the calorimetric measurements performed by the three different methods. The behaviour of the molar heat capacity over the entire temperature range studied is shown in Fig. 2a and demonstrates, firstly, the stability of the monoclinic phase $P2_1/c$ to a very

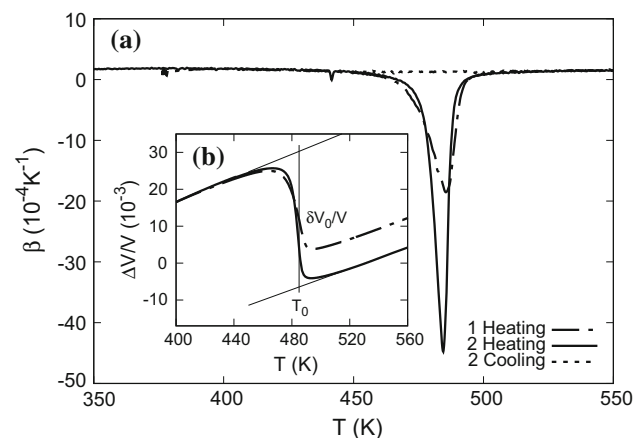


Figure 1 Temperature dependencies of thermal expansion coefficient β (a) and the volume strain $\Delta V/V$ (b) of K_2TaF_7 . Dashed line is lattice contribution $\beta_L(T)$ that coincides with the behaviour of $\beta(T)$ measured in cooling mode.

low temperature (4 K) and, secondly, the existence of only one strongly asymmetric heat capacity anomaly above room temperature, corresponding to the $Pnma - P2_1/c$ phase transition. The temperature of the maximum $C_p(T)$, $T_0 = 486.2 \pm 0.5$ K, agrees well with the value of the phase transition temperature found in dilatometric measurements and turned out to be slightly lower than the T_0 observed in optical experiments on single crystals (503–508 K) [7]. To determine the hysteresis value δT_0 in the sample under study, we performed measurements using DSC. Figure 3 shows the temperature dependence of the DSC signal measured in heating and cooling modes. At a thermal cycling rate equal to $dT/dt = 5 \text{ K min}^{-1}$, the DSC peaks corresponding to a phase transition temperature were found at 484.5 ± 1 K and 447.5 ± 1 K upon heating and cooling, respectively. The observed value $\delta T_0 \approx 37$ K shows why a structural transformation was not detected in dilatometric experiments during the cooling process.

To get information about the entropy of the phase transition, it was necessary to separate the anomalous, ΔC_p , and lattice, C_L , contributions to the total heat capacity, C_p , of K_2TaF_7 .

This procedure was carried out using a simple model describing $C_L(T)$. The experimental data taken far from the transition point ($T < 300$ K and $T > 510$ K) were fitted using a linear combination of Debye and Einstein terms $C_L = K_D C_D + K_E C_E$, where

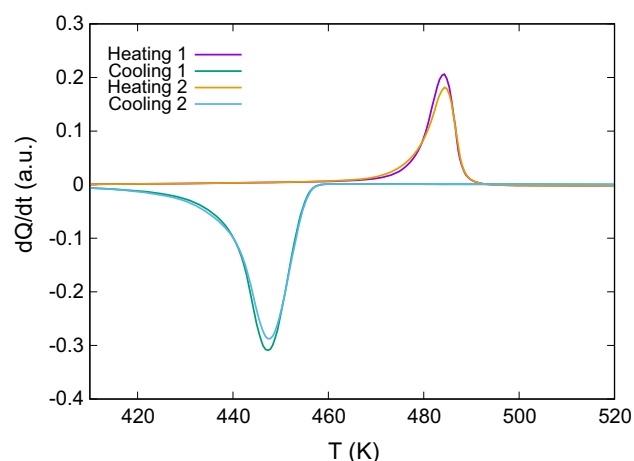


Figure 3 Temperature dependencies of dQ/dt measured in DSC experiments upon heating and cooling at the rate 5 K min^{-1} .

$$C_D(T) = 9R \left(\frac{T}{\Theta_D} \right)^3 \int_0^{\Theta_D/T} \frac{x^4 \exp(x)}{(\exp(x) - 1)^2} dx, \quad (1)$$

$$C_E(T) = 3R \left(\frac{\Theta_E}{T} \right)^2 \frac{\exp(\Theta_E/T)}{(\exp(\Theta_E/T) - 1)^2} \quad (2)$$

and K_D , K_E , Θ_D , and Θ_E are fitting parameters.

The average deviation of the experimental data from the smoothed curve does not exceed 1%. The lattice contribution is shown by a dashed line in Fig. 2a. The anomalous heat capacity, $\Delta C_p = C_p - C_L$, was observed over a very wide temperature range below the phase transition point $T_0 - 140$ K and correlates with the behaviour of the phase transition parameter [7].

Figure 2b demonstrates the temperature behaviour of the excess entropy associated with the phase transitions in K_2TaF_7 , determined by integration of the area under the ΔC_p versus T curve: $\Delta S_0 = 22.3 \pm 2.0 \text{ J (mol K)}^{-1}$. The entropy jump associated with the first-order phase transition was estimated to be approximately equal to $\delta S_0 = 14.5 \pm 2.0 \text{ J (mol K)}^{-1}$ (Fig. 2b).

Significant changes in entropy ($\Delta S_0 \approx R \ln 16$) and cell volume ($\delta V_0/V \approx 3.6\%$) during a phase transformation indicate that the distortions of the structure can be associated with order–disorder processes. However, the analysis of the structural data [9] showed that in the high-temperature phase, there is no disordering of any structural elements, the ordering of which could lead to an order–disorder transition. At the same time, in the $P2_1/c$ phase, the

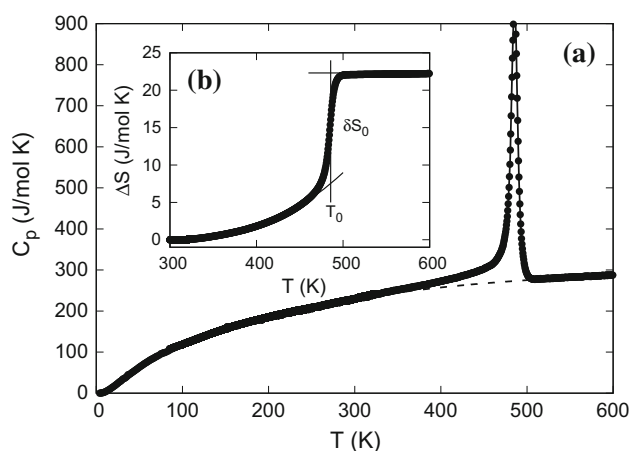


Figure 2 Temperature dependencies of the molar heat capacity (a) and anomalous entropy (b) of K_2TaF_7 . Dashed line corresponds to the lattice heat capacity C_L .

displacements of all atoms turned out to be anomalously large.

It can be assumed that the cause of the anomalously large entropy can be, firstly, a pronounced (but not extreme, leading to disordering) anharmonicity of the atomic vibrations in the *Pnma* phase and, secondly, the reconstructive nature of the transition accompanied by a giant jump in volume. It should be noted, however, that this is an unusual reconstructive transition, since the symmetries of the high-temperature and low-temperature phases are related to the group–subgroup relation.

Thus, the mechanism of the phase transition in K_2TaF_7 is very complex and remains uncertain to date.

Effect of hydrostatic pressure

Calorimetric and dilatometric studies have provided reliable evidence of the first-order phase transition in K_2TaF_7 . The susceptibility of transformations of this kind to hydrostatic pressure can be determined within the framework of the Clausius–Clapeyron equation, using the heat capacity and thermal expansion data

$$\frac{dT_0}{dp} = \frac{\delta V_0}{\delta S_0} = V_m \frac{\delta V_0/V}{\delta S_0}, \quad (3)$$

where V_m is the molar volume and δS_0 and δV_0 are the jumps in the entropy and volume at T_0 , respectively. Estimation of the derivative of the transition temperature with respect to pressure gives the value $dT_0/dp \approx -220 \pm 20 \text{ K GPa}^{-1}$.

To determine more accurately the magnitude of the baric coefficient, one can use the Pippard relation, which relates the temperature dependencies of the thermal expansion coefficient and heat capacity in the vicinity of the phase transition

$$C_p = \frac{V_m T_0}{\gamma} \beta + \text{const}, \quad \gamma = \frac{dT_0}{dp}. \quad (4)$$

Because the value of dT_0/dp is strongly dependent on the data close to the phase transition point, small errors in the temperature scales of the measurements of the heat capacity (the temperature sensor was a platinum thermometer) and thermal expansion (the temperature sensor was a thermocouple) will lead to significant errors in the results obtained using the Pippard relation. In this regard, the data on the thermal expansion and heat capacity were reduced to

one temperature scale by alignment of the phase transition temperatures.

The results of a joint analysis of the dependencies of $C_p(T)$ and $\beta(T)$ below T_0 are shown in Fig. 4. The experimental points fall on a straight line, which means that the Pippard relation is fairly well satisfied over a rather wide temperature range $T_0 - T = (5 - 35) \text{ K}$. Deviations from linear behaviour are observed near T_0 , where the imperfections of the sample, the dynamic mode of the thermal expansion measurements, and the difference in temperature scales for the measurements of $C_p(T)$ and $\beta(T)$ play a significant role. The obtained value of the baric coefficient $dT_0/dp \approx -212 \pm 15 \text{ K GPa}^{-1}$ agrees well with that calculated from the Clausius–Clapeyron equation and gives us hope that the value of dT_0/dp is close to the real one as well.

A negative sign and a large value of dT_0/dp indicate the possibility of a shift of the *Pnma* – *P2₁/c* phase transition to room temperature under a pressure of about 1 GPa. Due to the combination of the large values of ΔS_0 and dT_0/dp , the barocaloric efficiency of K_2TaF_7 turns out to be very high.

Barocaloric effect

The barocaloric effect is associated with a reversible change in entropy, ΔS_{BCE} , or temperature, ΔT_{AD} , of a thermodynamic system with a change in pressure under isothermal or adiabatic conditions, respectively. An important characteristic of barocaloric efficiency is also the minimum pressure, p_{min} , required to implement the maximum values of the

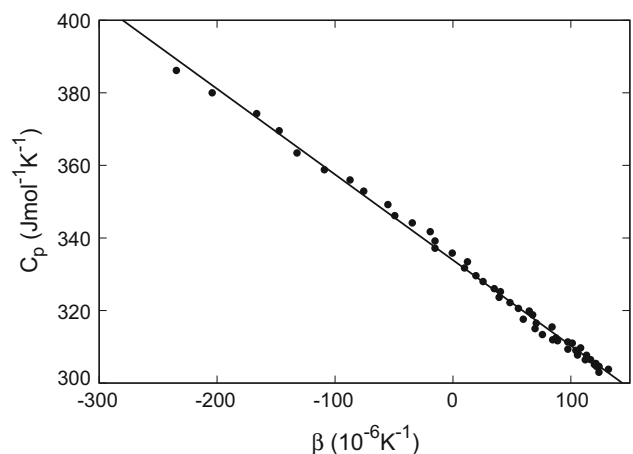


Figure 4 The relation between the molar heat capacity and the coefficient of volume thermal expansion below T_0 .

extensive, $\Delta S_{\text{BCE}}^{\text{max}}$, equal to the phase transition entropy, and intensive, $\Delta T_{\text{AD}}^{\text{max}}$, effects. In the case of a strictly first-order phase transition, the relations between these three parameters are as follows [12, 13]:

$$p_{\text{min}} \geq \frac{T\Delta S_0}{C_L dT_0/dp}, \quad \Delta T_{\text{AD}}^{\text{max}} \approx \frac{dT_0}{dp} p_{\text{min}} \quad (5)$$

Using the values C_L , ΔS_0 , and dT_0/dp determined above for K_2TaF_7 , we have found $p_{\text{min}} \approx 0.2$ GPa and $\Delta T_{\text{AD}}^{\text{max}} \approx -35 \pm 2$ K. The negative sign of the intensive BCE is associated with a decrease in the volume at the phase transition.

The behaviour of both the intensive and extensive BCEs with a change in pressure and temperature was analysed in the framework of the previously described method [14]. With this aim, the temperature dependencies of the total entropy under different pressures (Fig. 5a) were determined by adding the lattice entropy $S_L = \int (C_L/T)dT$ and the anomalous contribution $\Delta S(T)$ determined at $p = 0$ and shifted along the temperature scale according to the sign and value of dT_0/dp .

Recently, studies of differential thermal analysis under pressure for some complex fluorides and oxyfluorides revealed the absence of an effect of the pressure, at least to 0.6 GPa, on the phase transition entropy [14–16]. Taking into account these results, we assumed that also in the case of K_2TaF_7 , the pressure does not affect ΔS .

The behaviour of the extensive BCE determined using the temperature and pressure dependencies of the total entropy $\Delta S_{\text{BCE}} = S(T, p) - S(T, p = 0)$ is

shown in Fig. 6a. To obtain accurate information about $\Delta T_{\text{AD}}(T, p)$, the plots of $S(T, p) = S_L(T, p) + \Delta S(T, p)$ were analysed based on the condition of constant entropy $S(T, p) = S(T + \Delta T_{\text{AD}}, p = 0)$ (Fig. 6b).

In the first stage, we did not take into account the changes in the lattice entropy with pressure (Fig. 5a). The magnitudes of ΔS_{BCE} and ΔT_{AD} increase with increasing pressure, tending to maximum values, but not reaching them, at 0.5 GPa, which is higher than p_{min} (Fig. 6a, b). The difference between the estimated p_{min} and the experimental pressure is particularly associated with the validity of Eq. 5 for strong first-order phase transitions, whereas K_2TaF_7 undergoes a transformation close enough to the tricritical point. Nevertheless, the analysis showed the possibility of realizing very large values of both BCEs, $\Delta S_{\text{BCE}} \approx 21 \text{ J (mol K)}^{-1} = 54 \text{ J (kg K)}^{-1}$ and $\Delta T_{\text{AD}} \approx -30$ K, in this crystal at a rather low pressure $p \sim 0.5$ GPa. The intensive BCE is in good agreement with the maximum possible value $\Delta T_{\text{AD}}^{\text{max}}$ estimated above. It is necessary to point out that the intensive and extensive BCEs found in K_2TaF_7 are comparable and in some cases even exceed the barocaloric parameters in other materials [17–20].

On the other hand, the crystal lattice of potassium heptafluorotantalate is characterized by a positive volume deformation $\Delta V_L/V > 0$ and large volumetric thermal expansion coefficient $\beta_L \approx 1.5 \times 10^{-4} \text{ K}^{-1}$. In accordance with the Maxwell equation

$$\left(\frac{\partial S_L}{\partial p}\right)_T = -\left(\frac{\partial V_L}{\partial T}\right)_p, \quad (6)$$

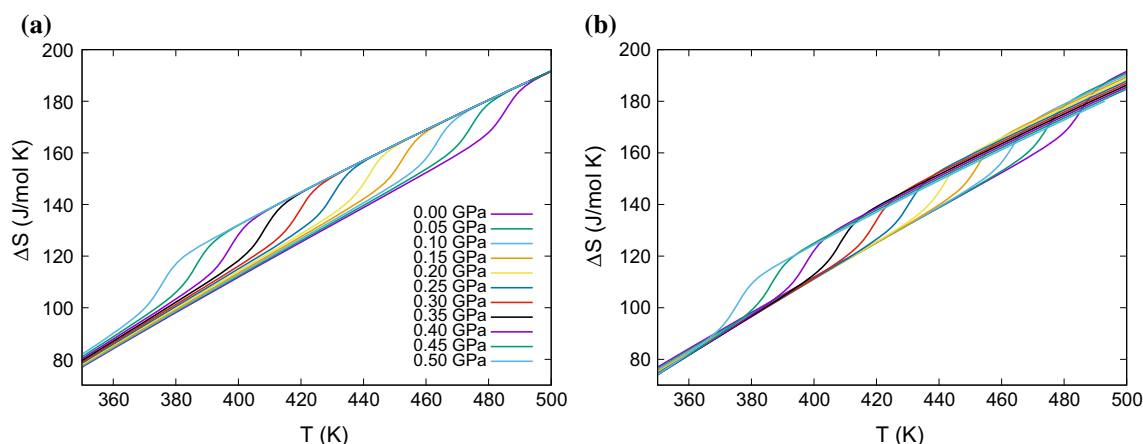


Figure 5 Temperature dependencies of total entropy of K_2TaF_7 at different hydrostatic pressures before (a) and after (b) correction for the additional lattice entropy changes with pressure.

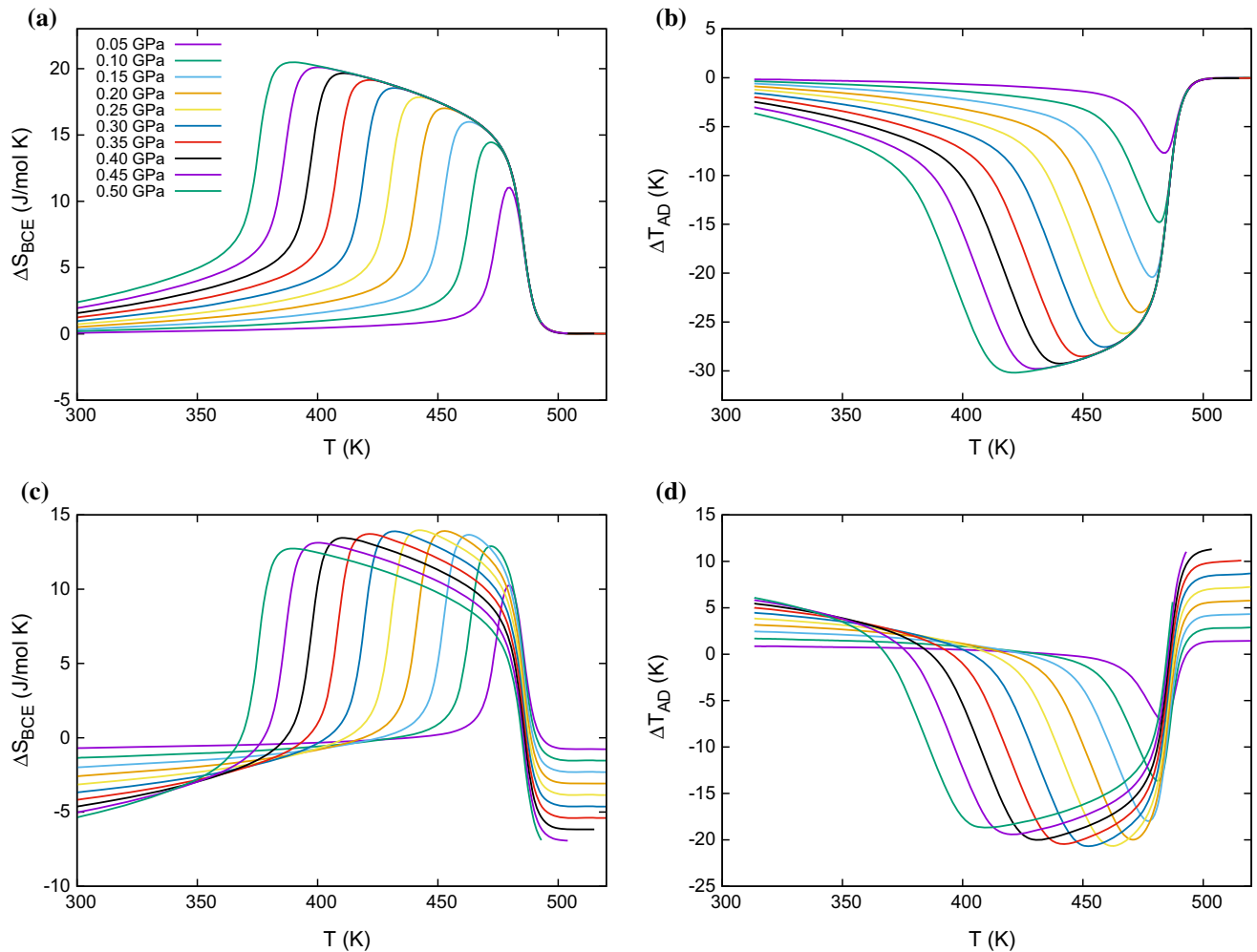


Figure 6 Temperature dependencies of barocaloric entropy and temperature changes at different hydrostatic pressures before (a, b) and after (c, d) correction for the additional lattice entropy changes with pressure.

this peculiarity leads to a significant conventional contribution ($\Delta S_{BCE}^L < 0$, $\Delta T_{AD}^L > 0$), associated with the expansion of the crystal lattice, to the total BCE, and as a result decreases the extensive and intensive inverse BCEs in the region of the phase transition.

Thus, to get detailed and accurate information about the BCE, it is necessary to know the pressure dependence of the total entropy. Due to a lack of opportunity to measure $C_p(T, p)$, the lattice entropy change with pressure, ΔS_L , may be expressed using Eq. 6 with S replacing by S_L :

$$\Delta S_L(T, p) = - \int_0^p (\partial V_L / \partial T)_p dp \approx -V_m \beta_L(T) p. \quad (7)$$

We assume here that the pressure does not significantly affect β_L and V_m .

Figure 5b shows the temperature dependencies of the total entropy at different pressures taking into account changes in the lattice entropy under pressure. The temperature and pressure dependencies of both the extensive and the intensive BCEs determined in this approximation are shown in Fig. 6c, d. It can be seen that in this case the behaviour of $\Delta S_{BCE}(T, p)$ and $\Delta T_{AD}(T, p)$ changed significantly and the peak values ΔS_{BCE}^{max} and ΔT_{AD}^{max} decreased. However, a rather large conventional BCE appeared above the transition temperature. As a result, at $p = 0.5$ GPa, there are very rapid changes in the values of ΔS_{BCE} (from -7 to $+14 \text{ J}(\text{mol K})^{-1}$ or from -18 to $+36 \text{ J}(\text{kg K})^{-1}$) and ΔT_{AD} (from $+12$ to -20 K). Recently, a similar effect of the lattice thermal expansion on BCE was observed in ferroelectric $(\text{NH}_4)_2\text{SO}_4$ [17].

The phenomenon of a change in the sign of BCE in a narrow temperature range was observed by us earlier in the vicinity of the triple points on the $T - p$ phase diagrams for a series of fluorides and oxyfluorides [12, 13]. The results obtained in the present paper and [12] are very important and promising from the point of view of searching for new materials with large BCE and designing original cooling cycles. It is obvious that in materials characterized by an increase in the volume of the unit cell during a phase transition, and a large value of the positive coefficient of volume thermal expansion far from the transition point, the BCE will increase due to the high compliance of the lattice entropy with the pressure.

Conclusions

Studies of the thermal expansion and the heat capacity of potassium heptafluorotantalate, K_2TaF_7 , performed over a wide temperature range, allowed us to establish the following important points.

Calorimetric measurements showed the stability of the phase $P2_1/c$ to a very low temperature (~ 4 K). The phase transition $P2_1/c - Pnma$ ($Z = 4$) is a pronounced first-order transformation accompanied by large values of thermal hysteresis ($\delta T_0 \approx 37$ K) and entropy ($\Delta S_0 = 22.3 \pm 2.0 \text{ J}(\text{mol K})^{-1}$) as well as jumps of the volume ($\delta V_0/V = -(3.6 \pm 0.5)\%$) and entropy ($\delta S_0 = 14.5 \pm 2.0 \text{ J}(\text{mol K})^{-1}$) at $T_0 = 486.2$ K. Anomalous behaviour of the heat capacity and entropy is observed over a very wide temperature range below the phase transition point $T_0 - 140$ K, which correlates with the behaviour of the parameter of the phase transition [7].

A very high sensitivity of the transition temperature to the hydrostatic pressure was found. Good agreement is observed between the values dT_0/dp determined using the Pippard ($-212 \pm 15 \text{ K GPa}^{-1}$) and Clausius–Clapeyron ($-220 \pm 20 \text{ K GPa}^{-1}$) equations. The large value and the negative sign of the baric coefficient indicate the possibility of a shift of the $Pnma - P2_1/c$ transformation to room temperature under a pressure of about 1 GPa.

Due to the combination of large values of ΔS_0 and dT_0/dp , K_2TaF_7 demonstrates very high barocaloric efficiency. It has been shown that the large thermal expansion of the crystal lattice leads to a large contribution of the conventional BCE to the total effect.

The conversion from the conventional BCE to the inverse is observed in a narrow temperature range and is accompanied by large changes in the intensive and extensive effects. These results show that the barocaloric efficiency can be increased in materials with conventional BCE and large positive values of β_L .

Acknowledgements

The reported study was funded by RFBR according to the research Project No. 18-02-00269_a.

Compliance with ethical standards

Conflict of interest The authors declare that they have no conflicts of interest.

References

- [1] Leblanc M, Maisonneuve V, Tressaud A (2015) Crystal chemistry and selected physical properties of inorganic fluorides and oxide-fluorides. *Chem Rev* 115:1191–1254
- [2] Mazej Z, Hagiwara R (2007) Hexafluoro-, heptafluoro-, and octafluoro-salts, and $[M_n F_{5n+1}]^-$ ($n = 2, 3, 4$) polyfluorometallates of singly charged metal cations, Li^+ , Cs^+ , Cu^+ , Ag^+ , In^+ and Tl^+ . *J Fluor Chem* 128:423–437
- [3] Laptash NM, Udovenko AA, Emelina TB (2011) Dynamic orientation disorder in rubidium fluorotantalate. Synchronous Ta-O and Ta-F vibrations. *J Fluor Chem* 132:1152–1158
- [4] Agulyansky A (2003) Potassium fluorotantalate in solid, dissolved and molten conditions. *J Fluor Chem* 123:155–161
- [5] Pogorel'tsev E, Mel'nikova S, Kartashev A, Gorev M, Flerov I, Laptash N (2017) Thermal, optical, and dielectric properties of fluoride Rb_2TaF_7 . *Phys Solid State* 59:986–991
- [6] Pogorel'tsev EI, Mel'nikova SV, Kartashev AV, Molocheev MS, Gorev MV, Flerov IN, Laptash NM (2013) Ferroelastic phase transitions in $(NH_4)_2TaF_7$. *Phys Solid State* 55:611–618
- [7] Mel'nikova SV, Bogdanov EV, Molocheev MS, Laptash NM, Flerov IN (2019) Optical and calorimetric studies of K_2TaF_7 . *J Fluor Chem* 222–223:75–80
- [8] Boča M, Rakhmatullin A, Mlynáriková J, Hadzimová E, Vasková Z, Mičušik M (2016) Differences in XPS and solid state NMR spectral data and thermo-chemical properties of iso-structural compounds in the series $KTaF_6$, K_2TaF_7

- and K_3TaF_8 and $KNbF_6$, K_2NbF_7 and K_3NbF_8 . Dalton Trans 44:17106–17117
- [9] Langer V, Smrčok L, Boča M (2006) Dipotassium heptafluorotantalate(V), β - K_2TaF_7 , at 509 K. Acta Cryst E 62:i91–i93
- [10] Torardi C, Brixner L, Blasse G (1987) Structure and luminescence of K_2TaF_7 and K_2NbF_7 . J Solid State Chem 67:21–25
- [11] Kartashev AV, Flerov IN, Volkov NV, Sablina KA (2008) Adiabatic calorimetric study of the intense magnetocaloric effect and the heat capacity of $(La_{0.4}Eu_{0.6})_{0.7}Pb_{0.3}MnO_3$. Phys Solid State 50:2115–2120
- [12] Gorev M, Bogdanov E, Flerov I (2017) T-p phase diagrams and the barocaloric effect in materials with successive phase transitions. J Phys D Appl Phys 50:384002
- [13] Gorev M, Bogdanov E, Flerov I (2017) Conventional and inverse barocaloric effects around triple points in ferroelastics $(NH_4)_3NbOF_6$ and $(NH_4)_3TiOF_5$. Scr Mater 139:53–57
- [14] Gorev MV, Flerov IN, Bogdanov EV, Voronov VN, Laptash NM (2010) Barocaloric effect near the structural phase transition in the Rb_2KTiOF_5 oxyfluoride. Phys Solid State 52:377–383
- [15] Pogorel'tsev E, Flerov I, Kartashev A, Bogdanov E, Laptash N (2014) Heat capacity, entropy, dielectric properties and T-p phase diagram of $(NH_4)_3TiF_7$. J Fluor Chem 168:247–250
- [16] Flerov IN, Kartashev AV, Gorev MV, Bogdanov EV, Mel'nikova SV, Molokeev MS, Pogorel'tsev EI, Laptash NM (2016) Thermal, structural, optical, dielectric and barocaloric properties at ferroelastic phase transition in trigonal $(NH_4)_2SnF_6$: A new look at the old compound. J Fluor Chem 183:1–9
- [17] Lloveras P, Stern-Taulats E, Barrio M, Tamarit JL, Crossley S, Li W, Pomjakushin V, Planes A, Mañosa L, Mathur ND, Moya X (2015) Giant barocaloric effects at low pressure in ferroelectric ammonium sulphate. Nat Commun 6:8801
- [18] Mañosa L, González-Alonso D, Planes A, Bonnot E, Barrio M, Tamarit JL, Aksoy S, Acet M (2010) Giant solid-state barocaloric effect in the Ni-Mn-In magnetic shape-memory alloy. Nat Mater 9:478–481
- [19] Mañosa L, González-Alonso D, Planes A, Barrio M, Tamarit JL, Titov IS, Acet M, Bhattacharyya A, Majumdar S (2011) Inverse barocaloric effect in the giant magnetocaloric La-Fe-Si-Co compound. Nat Commun 2:595
- [20] Yuce S, Barrio M, Emre B, Stern-Taulats E, Planes A, Tamarit JL, Mudryk Y, Gschneidner KA, Pecharsky VK, Mañosa L (2012) Barocaloric effect in the magnetocaloric prototype $Gd_5Si_2Ge_2$. Appl Phys Lett 101:071906

Publisher's Note Springer Nature remains neutral with regard to jurisdictional claims in published maps and institutional affiliations.